UPPSALA
UNIVERSITET

UPTEC F 10021
Examensarbete 30 hp
Juni 2015

X-Ray Photoemission Spectroscopy Characterization of Fe(II)- and Fe(III)-Phthalocyanine Molecular Films

Sonja Droschke

UPPSALA
UNIVERSITET

Teknisk- naturvetenskaplig fakultet
UTH-enheten

Besöksadress:
Ångströmlaboratoriet
Lägerhyddsvägen 1
Hus 4, Plan 0

Postadress:
Box 536
751 21 Uppsala

Telefon:
018 – 471 30 03

Telefax:
018 – 471 30 00

Hemsida:
http://www.teknat.uu.se/student

Abstract

X-Ray Photoemission Spectroscopy Characterization of Fe(II)- and Fe(III)-Phthalocyanine Molecular Films

Sonja Droschke

This thesis investigates the electronic structure of iron phthalocyanine (Fe(II)Pc) and iron phthalocyanine chloride (Fe(III)PcCl) immobilized on surfaces. For this purpose two different deposition methods are used and compared: smearing the molecular powder under atmosphere condition and evaporation of a molecular layer in ultra-high vacuum. The electronic states of FePc and FePcCl are probed with photoelectron spectroscopy (PES) and compared in relation to the ionic state of the central metal (Fe). The PE spectra show that evaporation of FePcCl at around 350°C results in dissociation of the chlorine from the FePc molecule, which is stable at this temperature. Mass spectroscopic measurements during heating of FePcCl in ultra-high vacuum (UHV) show a clear Cl signal for temperature still below 250°C. Theoretical calculations of the binding energy for Cl in FePcCl seem to indicate dissociation of the Cl from the molecules.

Handledare: Joachim Schiessling
Ämnesgranskare: Carla Puglia
Examinator: Tomas Nyberg
ISSN: 1401-5757, UPTEC F 10021

1 Introduction 4

2 Phthalocyanines 5

3 Experimental set-up and technique 6

3.1 Principles of photoelectron spectroscopy 6
3.2 Chemical shift 7
3.3 Experimental equipment 7
3.4 The evaporation chamber 8

4 Sample preparation 10

4.1 Substrates 10
4.2 Deposition 10
4.3 Adsorbates 11
4.3.1 Iron(II) phthalocyanine 11
4.3.2 Iron(III) phthalocyanine chloride 12

5 Results and discussion of XPS data 13

5.1 C 1s spectra 13
5.2 N 1s spectra 14
5.3 Fe 2p spectra 15
5.4 Cl 2p spectra 16

6 Results and Discussion of Mass Spectrometer Data 19

7 Discussion 24

8 Summary and Conclusions 28

9 Bibliography 29

1 Introduction

Nature has always been a source of inspiration when seeking for new technical solutions. Mankind's attempt to imitate nature is nowadays called biomimetics[1] (from the Greek words βιοσ (life) and μιμοσ (to mime)).

Already in the Greek mythology, Daidalos constructs "flying devices" by imitating bird wings to escape his prison. More recently, in 1948, the Swiss engineer George de Mestral invented the Hook and Loop fastener Velcro after studying annoying burrs. The investigation of lotus flowers led to the discovery of the lotus effect[2] that made it possible to develop surfaces that can stay clean and dry themselves.

Even this work is based on the aim to imitate nature, especially enzymes.

Enzymes are organic macromolecules functioning as catalysts in biological processes. They are generally reaction-, substrate- and regio-specific making them highly efficient. They can run a reaction over and over again as they are left unaltered after the catalytic reaction. The disadvantage with enzymes is that they are sensitive to thermal and chemical changes in the surrounding.

One group of catalysts used in biomimetics are porphyrins which are also found in the active site of many enzymes, as the two well-known examples of chlorophyll and haemoglobin.

Purely artificial compounds called phthalocyanines (Pc's) are built up in a structure similar to the natural porphyrins. However phthalocyanines showed to be very stable both chemical and thermal in contrast to porphyrins. Therefore phthalocyanines became of special interest for biomimetic applications.

It is already common to use phthalocyanines in homogeneous catalysis (where the reactants and their products are in solution) for many industrial applications.

Even though such homogenous processes are widely used, improvements are highly desired for increasing the lifetime of the catalysts and to overcome the difficulty to separate products from the catalysts. The immobilization of the catalytic molecules (Pc's) on surfaces [1], (i.e. to use them in heterogeneous catalysis), has already shown to solve the separation problem and to improve the lifetime since the molecules, bonded on a surface, cannot form dimers or clusters which are the cause of the short lifetime of the homogeneous catalysis process.

The aim of this work was to study the electronic structure of iron phthalocyanines deposited on surfaces in relation to the ionic state of the central metal (Fe). Therefore we have studied Fe(II)Pc and Fe(III) PcCl. Different deposition methods have been used and compared. Our results show that evaporation of FePcCl results in dissociation of the chlorine from the FePc molecule.

[1] The term biomimetics was coined in the 1950s. Other words used for it are bionics, biomimicry and biognosis.

[2] Discovered in 1997 by W. Barthlott and C. Neinhuis

2 Phthalocyanines

Phthalocyanines are macrocyclic compounds that do not exist in nature but were accidentally discovered in laboratories as a by-product in 1907 [2] and as a copper salt in 1927 [3].

In the 1930s phthalocyanines became very interesting for industrial use as dye. Their colours are strong, bright blue to green and do not fade in sunlight. In the last two decades they even became important commercially as photoreceptor in laser beam printers and photocopiers.[4] Pc's are used in fuel cells, solar cells, radiation sensors, electronic components and in medicine e.g. in cancer therapy [5][6][7][8][9].

Although the molecular structure of metal-free and metal phthalocyanines was soon discovered (1934) [10] there are still ongoing investigations about the single-crystal and solid-state structure of phthalocyanine molecular films for relating it to the many physical properties characteristic for each application.

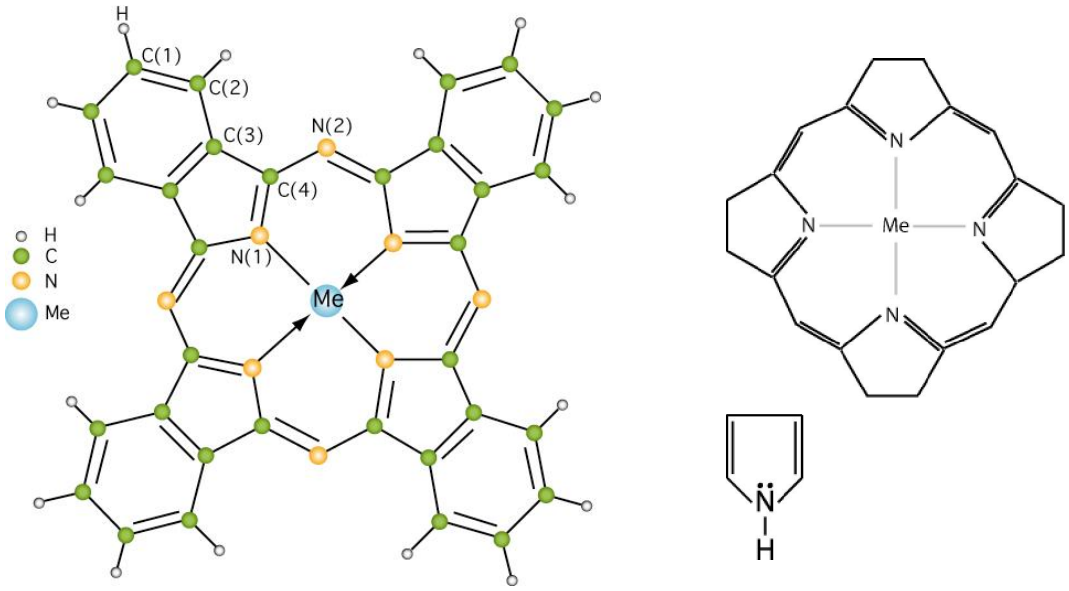

Figure 2-1: Metal phthalocyanine (left), metal porphyrin ring and a pyrrole group

Phthalocyanines have a porphyrin like structure. Porphyrin consists of four pyrrole units (C_4H_5N) linked by four methine bridges (-CH-). (See Figure 2-1).

Phthalocyanine ($C_{32}H_{18}N_8Me$) instead consists of four pyrrole units with four carbons attached in ring structure (benzene) linked together by N bridges[3]. In the centre of the ring structure one can find two H atoms (metal-free Pc) or a metal ion (metal Pc), usually a transition metal from the first transition series[4] in the periodic system [11]. The bonds in the molecule are covalent bonds[5]. The central atom coordinates with the pyrrole nitrogen atoms. (See Figure 2-1).

Phthalocyanines crystallize by forming stacks of molecules. The interaction between the molecule layers is weak, mediated by van der Waals forces.[12]

[3] The nitrogen bridges are also called aza-bridges. Phthalocyanine is therefore sometimes called an azaporphyrin.
[4] The transition metals of the first transition series are Ti, V, Cr, Mn, Fe, Co, Ni, Cu, Zn
[5] In a covalent bond atoms share one or more electron pairs.

3 Experimental set-up and technique

The experimental technique used in this study is known as core level (CL) photoelectron spectroscopy (PES). It can deliver information about the chemical composition of a sample and for this reason PES is also called ESCA - Electron Spectroscopy for Chemical Analysis.

ESCA is based on the information gained by photoelectrons emitted from the sample under x-ray excitation. This technique is also known as XPS (X-ray Photoelectron Spectroscopy). It was developed in the late 50's at Uppsala University by K. Siegbahn and his group [13]. XPS is a surface sensitive method probing the energy levels of inner shell (=core) electrons. XPS does not only give us information on the chemical composition of a sample but probes even the oxidation states of the atoms in the sample and molecule-surface interactions between sample and carrier.

3.1 *Principles of photoelectron spectroscopy*

When a sample is irradiated with x-rays of sufficient high energy, it will emit electrons, called photoelectrons[6]. Using the law of energy conservation one can obtain the kinetic energy of the emitted photoelectron by $E_k = h\nu - E_b - \varphi$, where $h\nu$ is the energy of the incoming x-ray, E_b is the binding energy of the electron with regard to the Fermi level and φ is the work function (energy between vacuum level and Fermi level). Every element of the periodic table has its distinct set of binding energies for its electrons. This makes it possible to identify an atom chemically by its photoelectron spectrum, i.e. to get a chemical analysis of a sample.

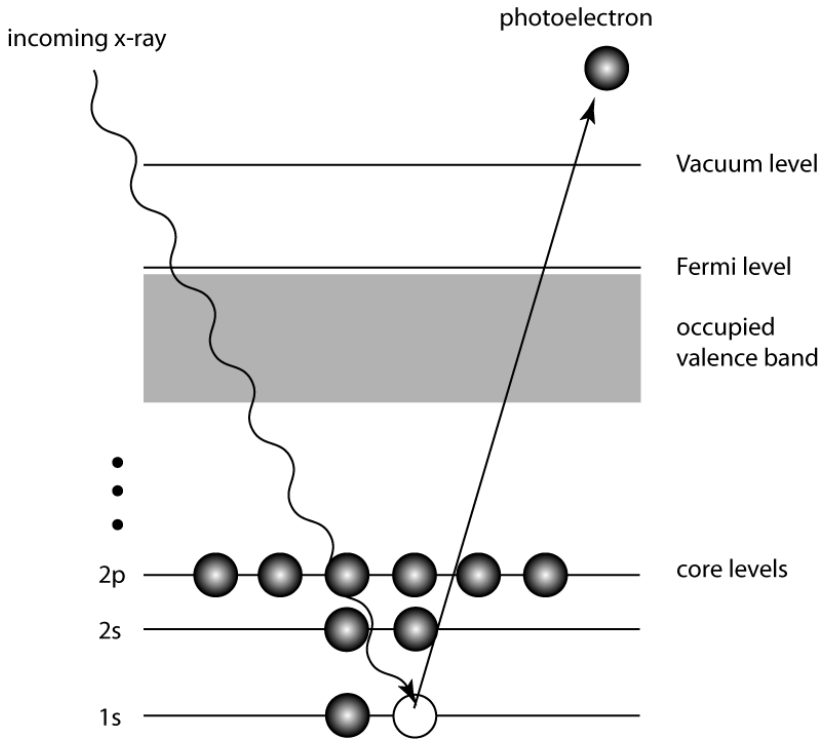

Figure 3-1: The incoming light is absorbed by a core electron that leaves the atom as a so-called photoelectron.

[6] The emission of photoelectrons, also known as the photoelectric effect was described by A. Einstein in 1905 and earned him the Nobel prize in 1921.

3.2 *Chemical shift*

As mentioned before, distinct binding energies for the electrons are unique for every element of the periodic table allowing the chemical analysis of a sample by its photoelectron spectrum. However the binding energy of a core level can shift with respect to that of a pure atom. If the atoms are part of a chemical compound electrons of the outer shell(s) (= valence levels) take part in the chemical bonding. Even though the core level electrons do not participate in chemical bonding, they feel a change in the charge distribution around them due to the redistribution of the valence electrons. The core electrons react then by adjusting their binding energies to the new chemical environment. This effect is called chemical shift, which can result in a binding energy shift between meV to some eV. This shift gives us more complete information about the electronic structure (e.g. the oxidation states of the atoms) and the geometrical structure of the compound system.

3.3 *Experimental equipment*

The instrument used to analyse the samples is a VG Scienta SES 200 spectrometer in the ESCA200 Laboratory at the Department of Physics and Astronomy at Uppsala University.

The ESCA instrument consists of two main parts: a source, generating x-rays for irradiation of the sample, and an electron spectrometer for the analysis of the electrons emitted from the sample [14].

Figure 3-2 shows a schematic sketch of the ESCA instrument used for this study.

The x-ray source consists of an electron gun, a rotating aluminium coated titanium alloy anode and a monochromator consisting of seven crystals. The monochromator selects the Al Kα line (=1486.7 eV) [15] which is focused onto the sample by arranging the exit slit for the radiation from the anode, the monochromator and the sample on a Rowland circle. The Al Kα radiation is used for excitation of the sample.

The emitted photoelectrons enter into the electron spectrometer. First they pass an electronic lens system for retarding and focusing of the incoming electrons and then they continue through an adjustable entrance slit. Next follows the hemispherical electron analyser with radius of 200 mm (SES200) for the main trajectory. A detector consisting of multi-channel plates, a fluorescence screen and a CCD camera records the events of incoming electrons.

The energy resolution of the spectrometer can be calculated by the following formula:

$$\Delta E[eV] = \frac{E_p d}{2 r_A}$$

r_A = radius of the hemispherical analyser (200mm)
E_p = pass energy (300/150/75eV)
d = size of the entrance slit (0.8mm)

The spectra shown in this work were recorded at a pass energy of 300 eV. The energy resolution of the spectra is thus ΔE= 0.6 eV. All spectra were taken at a take-off angle of 90°.

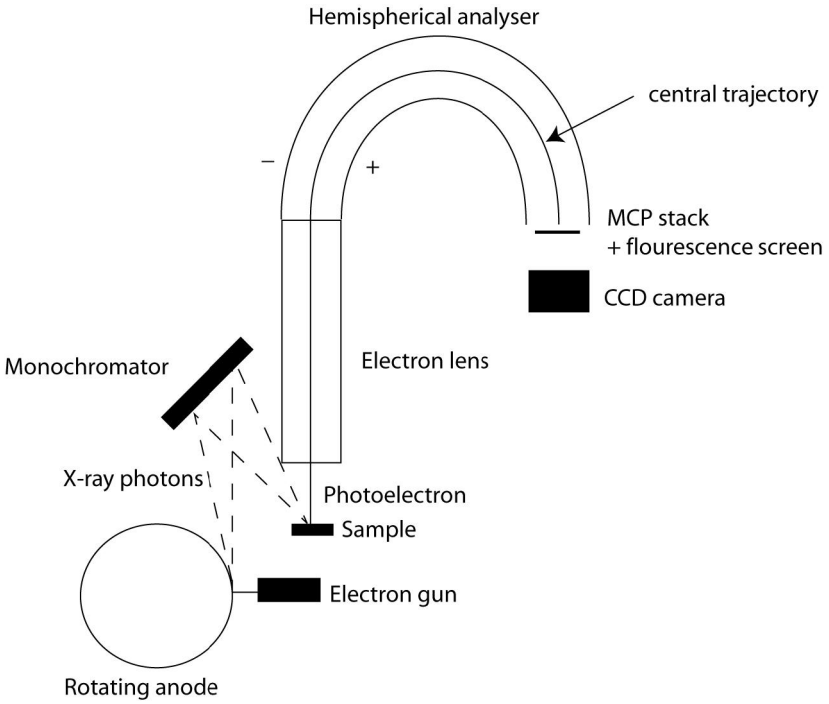

Figure 3-2: A schematic sketch of the ESCA instrument. The photoelectrons are sorted by their kinetic energy in a radial electrostatic field created by two concentric hemispheres in the analyser. The trajectories of electrons with high kinetic energy are bent less than those with lower energy. Electrons of different kinetic energy are thus spatially resolved on the detector. The kinetic energy of electrons passing the analyser on the central trajectory is called the pass energy of the spectrometer. Electrons within ±5% of the pass energy are able to reach the detector. High pass energy means lower energy resolution and vice versa. To be able to cover a large energy range for a fixed pass energy the entering electrons pass an electron lens system where they can be accelerated or decelerated to fit the set pass energy before entering the electromagnetic field between the hemispheres. The resolution of the spectrometer is also influenced by the size of the entrance slit. A smaller slit will let in fewer electrons from the interaction region and lower the intensity but it will result in a better spectral resolution. The recording of the electrons passing through the analyser is done by a detector consisting of two micro channel plates working as a secondary electron multiplier, a fluorescence screen and a CCD camera.

3.4 *The evaporation chamber*

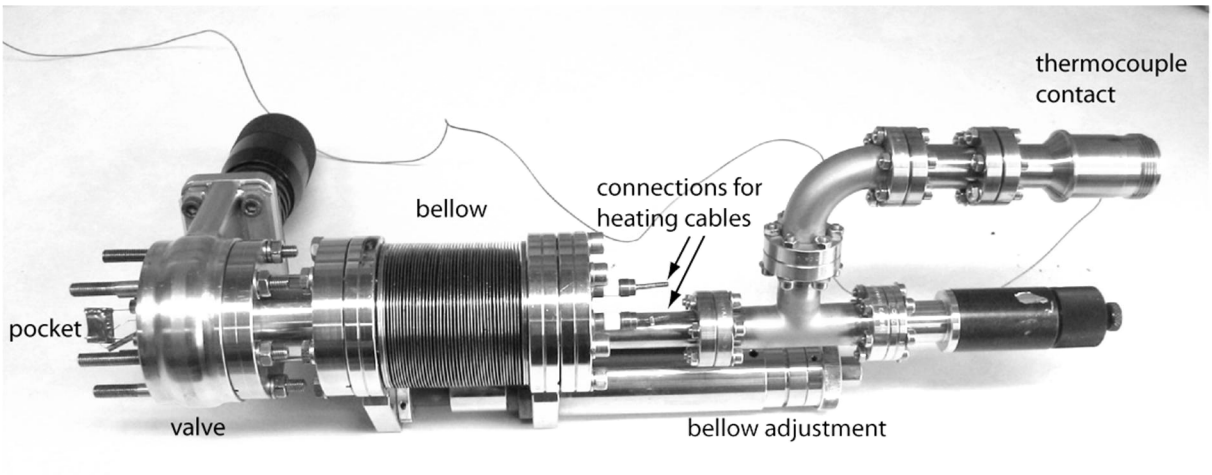

Figure 3-3: The evaporator detached from the deposition chamber

The evaporator consists of a tight pocket of tantalum foil where the chemicals[7] are enclosed. Two tungsten wires are attached to the pocket as contacts for the current supplied for heating. The evaporation chamber is a vacuum system consisting of the evaporator on a linear translator and a deposition chamber.

For molecular deposition on the sample surfaces, the evaporator pocket is lowered into the deposition chamber where the substrates are placed. When the evaporation temperature (between 350 and 400°C) is reached a clean molecular vapour emerges through a small hole at the bottom of the pocket allowing deposition of the molecules on the substrates.

The pressure in the chamber during deposition was in the $1*10^{-6}$ mbar range with a maximum of $2.0*10^{-6}$ mbar.

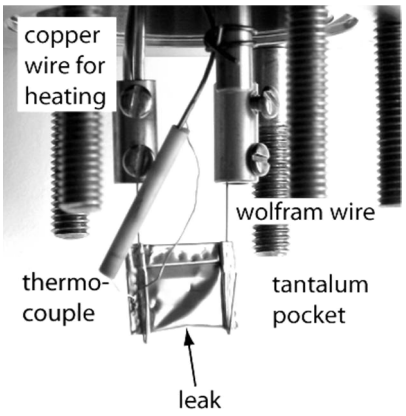

Figure 3-4: Pocket mounted in the evaporator. Three edges of the pocket are double folded and point welded to ensure tight enclosure of the substance.

[7] More about the used chemicals in chapter 4.3.

4 Sample preparation

The samples that we have characterized in this study consisted of molecular films adsorbed (i.e. deposited) onto surfaces (substrates).

The adsorption of molecules on surfaces can be of different character, physical (physisorption), chemical (chemisorption) or in between considering that there is no clear and distinct edge between these kinds of interactions. In the case of pure physisorption the molecules are bound to the surface by the weakest way of interaction, van der Waals forces. In chemisorption instead the molecules form a chemical bonding with the surface atoms by forming covalent or ionic bonds. Moreover, the adsorption strength and geometry often depend on the deposition method used.[16]

4.1 *Substrates*

The substrates used for most samples were of transparent, conducting oxide coated glass (TCO glass), coated on one side with fluorine-doped tin oxide (SnO_2:F), also called FTO glass. This oxide layer is electrical conducting which helps to avoid sample charging during XPS measurements.

The FTO glass was cut into small bits of around 8x10 mm^2 to fit the sample holders for the XPS system. Then the glass plates were thoroughly cleaned in isopropanol in an ultrasonic bath for 10 to 15 min. Afterwards they were dried under an argon stream and immediately moved for further preparation into the analysis chamber.

One more type of sample was prepared depositing the molecular films directly on a sample holder plate, consisting of a tantalum plate, cleaned in the same way as the glass substrates prior to deposition.

4.2 *Deposition*

For deposition of the FePc molecules, two different techniques were used. For *ex situ* samples the molecular powder was simply smeared onto the substrate with a stainless steel spatula. For the *in situ* samples the molecules were deposited in vacuum on the substrate by evaporation inside the evaporator chamber described in chapter 3.4.

Sample A, B and D were prepared with the *ex situ* technique. Sample C was prepared *in situ* but had to be in atmosphere during mounting on the sample holder for transferring it into the XPS equipment.

All glass samples needed to be mounted on a sample holder that would fit the transfer system of the XPS. The holders are plates made of pure tantalum or molybdenum. Before each mounting, the holders were cleaned in the same way as the glass substrates, 10-15 min ultrasonic bath in isopropanol. The mounting took between five to ten minutes.

Four characteristic samples were picked to illustrate the data, further on denoted as follows:

Sample A: FePcCl *ex situ* thin film
Sample B: FePcCl *ex situ* thick film
Sample C: FePcCl *in situ* thick film
Sample D: FePc *ex situ*

For the *ex situ* films the terms thick and thin are used to distinguish the thickness of the deposited films. This should not be interpreted as absolute values as the actual thickness of the molecular films has not been measured. I chose this denotation to put two films in relation to each other. It was visible by eye that “thick” films consisted of much more material than

"thin" layers. I denoted films as "thin" when the glass substrate was visibly light green coloured by the Pc molecules but still transparent. A "thick" film was heavily dark green and the glass appeared opaque at many spots.

For sample D the substrate as mentioned was a sample holder of tantalum

4.3 *Adsorbates*

Two different molecules were used as adsorbates: Fe(II)Pc and Fe(III)Pc(Cl). Both were bought from Sigma-Aldrich[8] and came in salt-form in small glass bottles. Aldrich states a dye content of 90% for Fe(II)Pc respectively 95% for Fe(III)Pc(Cl).

4.3.1 Iron(II) phthalocyanine

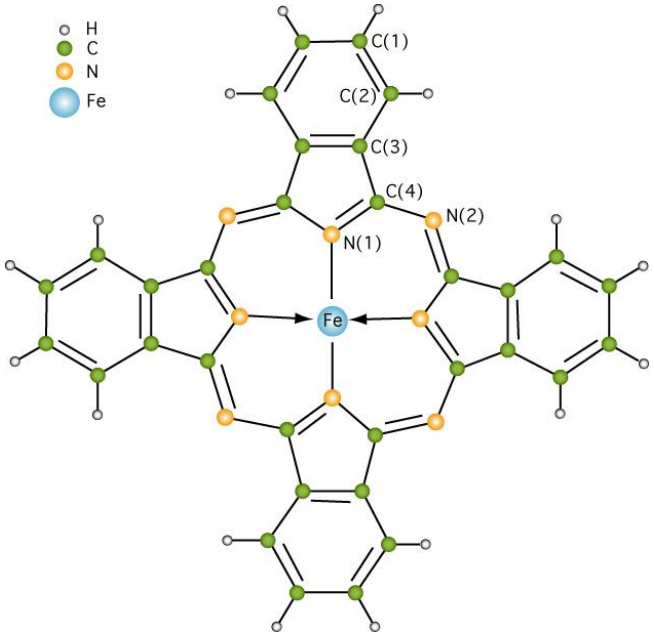

Figure 4-1: Iron phthalocyanine in the xy-plane

The molecular structure of iron phthalocyanine[9] (FePc) is symmetric to the central atom. It spreads out in a two-dimensional xy-plane and is planar in z-direction. The colour of FePc is blue. The oxidation state of the iron is formally Fe^{2+}. The effective atomic charge of the iron is calculated to 0.71 pointing at a significantly covalent and not purely ionic bonding between the Fe atom and the Pc molecule. The bonding of the Fe atom to the ring is very strong, calculated to E_{bind} = -9.81 eV. [17] A synonym for iron phthalocyanine is phthalocyanine iron(II) salt.

[8] www.sigma-aldrich.com
[9] Chemical formula: $C_{32}H_{16}FeN_8$

4.3.2 Iron(III) phthalocyanine chloride

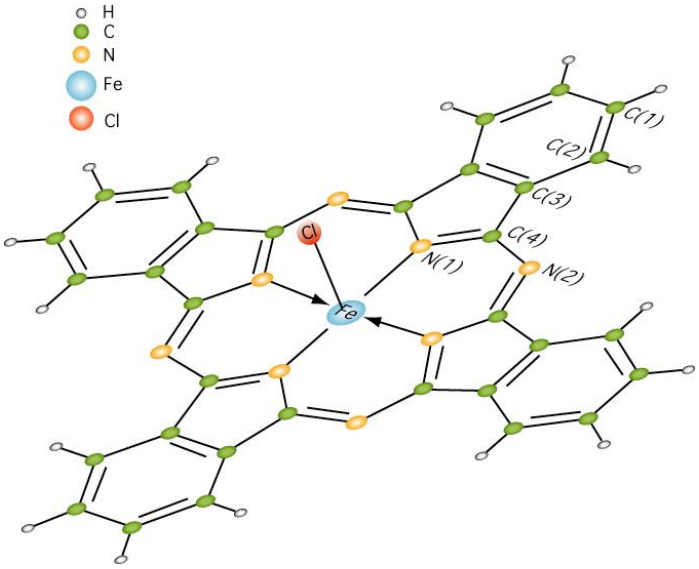

Figure 4-2: Iron(III) phthalocyanine chloride, FePcCl

The molecular structure of iron(III) phthalocyanine chloride[10] (FePcCl) is symmetric through the central atom in the xy-plane. But unlike FePc the molecule is not flat but has a component in z-direction represented by the Cl atom attached to the central Fe atom. The chlorine reduces Fe^{2+} in FePc to Fe^{3+} in FePcCl. The difference in oxidation state is even indicated in a colour change. FePcCl appears dark green whereas, as mentioned the FePc is dark blue. A synonym for iron(III) phthalocyanine chloride is phthalocyanine iron(III) monochloride salt and sometimes FePcCl can be denoted as (chloro)phthalocyaninatiron(III) complex, abbreviated as FeCl(Pc), in literature.

The ground state of the electronic configuration of reduced FePc (e.g. FePcCl) remains still in doubt and it is discussed whether actually the metal (Fe) or the ligand (Cl) is oxidized.[17]

[10] Chemical formula: $C_{32}H_{16}ClFeN_8$

5 Results and discussion of XPS data

In this chapter I will present the XPS spectra for the different samples taken at the C 1s, N 1s, Fe 2p and Cl 2p binding energy regions. The data have been compared with the aim to understand the electronic structure of the different molecules used (Fe(II)Pc and Fe(III)Pc) as well as of the molecular films obtained by the different deposition methods.

To limit radiation damages, the samples were moved after a couple of runs in order to expose another spot to the x-ray beam. Due to the preparation method the *ex situ* samples show to be inhomogeneous in film thickness. These may lead to charging effects during XPS measurements. As we cannot exclude the possibility of charging it raises problems in interpretation of the energy shifts observed in the spectra. In the following discussion we have mainly focussed on the line profiles more than the binding energy positions due to the lack of a reliable reference line for the binding energy scale calibration.

The spectra shown are taken at 300 eV pass energy which results in an energy resolution ΔE=0.6 eV.

5.1 *C 1s spectra*

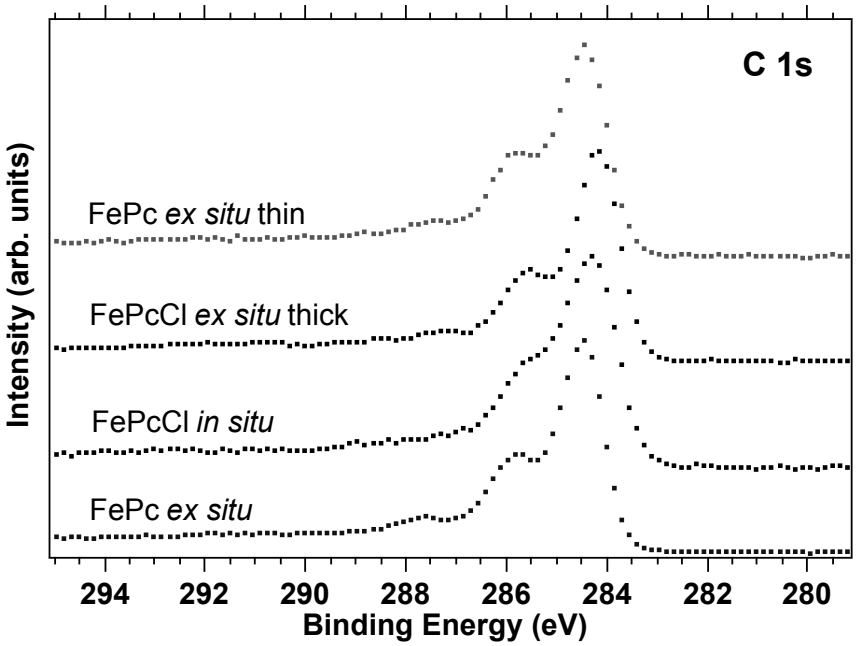

Figure 5-1: C 1s x-ray photoemission spectra for the different kinds of samples.

At first sight, we can see three contributions to the C 1s spectrum. The highest peak at approximately 284.4 eV stems from the 24 carbon atoms in the benzene rings. The second highest peak is observed at about 285.6 eV and comes from the eight pyrrole carbons. At around 287.5 eV we see the third contribution to the spectrum, a low intensity structure that as explained by Åhlund et al. is due to shake-up electron transitions mostly from pyrrole carbons. [18]

Another intensity, shake-up contributions of electrons from benzene atoms, is hidden under the pyrrole peak. This explains why the expected intensity ratio of 1:3 between the signals of the 8 pyrrole and the 24 benzene carbons is not observed. [19]

The difference in binding energy between carbon atoms in pyrrole and benzene is about 1.3 eV for all samples investigated.

The dip between the C 1s benzene and pyrrole peaks for evaporated FePcCl is not as deep as expected for FePc. This could be due to the different molecular structure between the FePc and the FePcCl and/or to different geometric organizations of the molecules causing a different kind of molecule-molecule interactions. However we could also consider this result as due to contaminations and the poor experimental resolution.

5.2 *N 1s spectra*

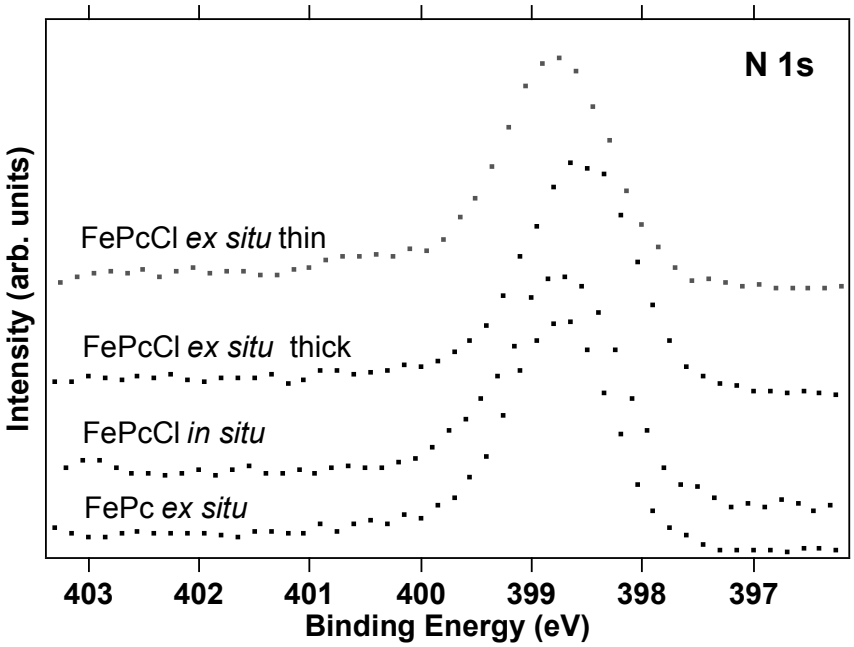

Figure 5-2: N 1s XPS spectra

The N1s spectra show a peak at about 398.7 eV and some additional low intensity structures at higher binding energies, around 400 eV and 405 eV. Although we have two energetically different positions for nitrogen atoms in the molecule there is only one N 1s peak. This is explained by Åhlund et al. [18] by theoretical calculations that show that the two chemically non-equivalent N atoms result in two peaks shifted only 0.3 eV in binding energy, which is beneath the energy resolution of the presented spectra.

The spectrum of the *in situ* FePcCl sample shows a slightly broader line shape than the others. For *ex situ* samples we see no difference in line shape between FePc and FePcCl.

These data show that the Cl atom is not influencing the N atoms in the molecules. We know that the HOMO of the FePc molecules has mostly C 2p character whereas the Fe 3d states give most contributions to the HOMO-1 orbital. [20] We could then expect that the Cl atom would mostly influence such molecular orbitals affecting then mainly the C and Fe core line spectra.

5.3 *Fe 2p spectra*

The Fe 2p spectra consist of two peaks, one asymmetric peak at around 711 eV coming from electrons of the Fe $2p_{3/2}$ level and another less intense peak at approximately 724 eV from Fe $2p_{1/2}$ electrons. For all FePcCl spectra we record another peak in between the 2p-orbital peaks due to tin from the glass substrate, the Sn $3p_{3/2}$ peak at 717 eV. As mentioned before the FePc *ex situ* sample was prepared on a tantalum plate and thus does not show a tin peak. There should be satellite peaks accompanying the two Fe 2p peaks and giving further information about the oxidation state of the iron atom, but, unfortunately, we cannot observe them in these spectra. [21] In the case of Fe 2p spectra for FePcCl the Sn $3p_{3/2}$ peak is shading the area where the satellite might be observed and the FePc spectrum is not clear either in this region.

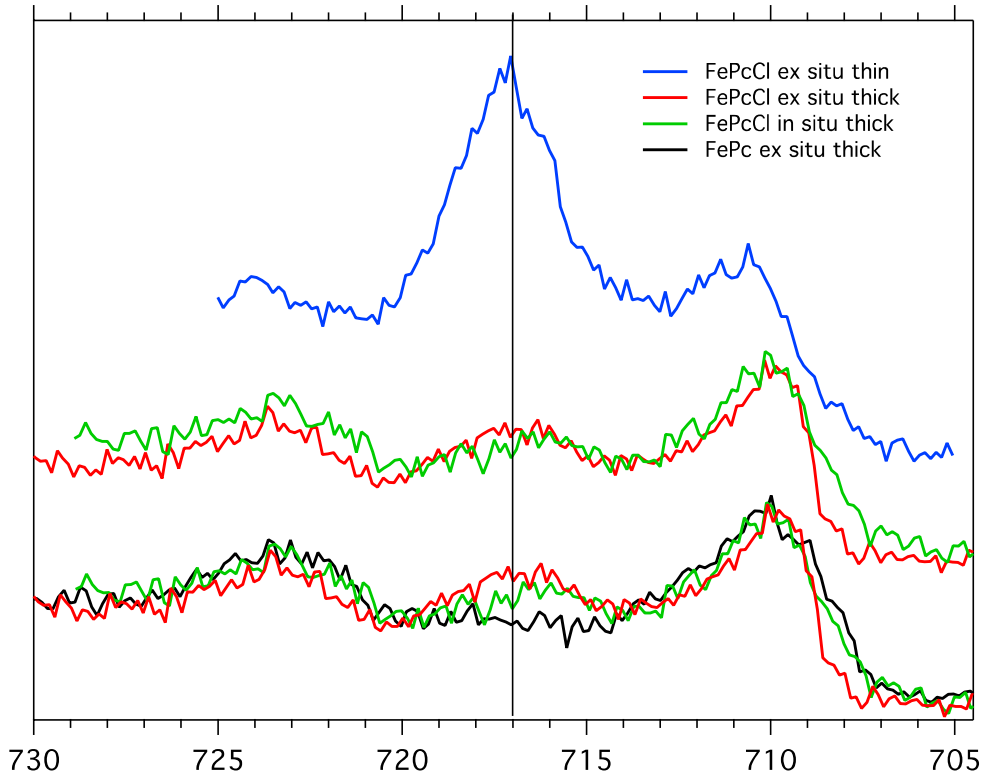

Figure 5-3: Fe 2p XPS spectra. Comparison between *in situ* and *ex situ* films of FePcCl and FePc. The vertical line indicates the binding energy of the Sn3p3/2 line (717 eV).

When comparing the Fe 2p spectra of FePcCl and FePc (Figure 5-3) I will limit the discussion to the line profiles omitting a comparison of the possible binding energy shifts, which actually could evidence quite interesting effects related to the different Fe ionic states. The reason for this, as already mentioned, has been the difficulties we met in our experiments, lacking a common reference line for calibration of all the samples, i.e. of FePc and FePcCl films. In the comparison shown in Figure 5-3 I have just aligned the Sn $3p_{3/2}$ peaks at 717 eV binding energy, visible in all the spectra of FePcCl films.

Then we can make the following observations:
1. The comparison of the *in situ* and *ex situ* thick films of FePcCl shows that the Fe $2p_{3/2}$ line for the *ex situ* sample is narrower (red and green lines in Figure 5-3).
2. The *ex situ* prepared film of FePc (black line) shows a Fe $2p_{3/2}$ line very similar to the thin *ex situ* (blue line*)* and thick *in situ* (green) line of FePcCl films.

3. The *in situ* thick and *ex situ* thin film of FePcCl are very similar in line profiles.

By just comparing the *in situ* thick with the *ex situ* thick film of FePcCl we can conclude that something happens when passing from *ex situ* to *in situ* preparation of FePcCl films. I will discuss this result more in the following sections together with the Cl 2p spectra and the mass spectrometry measurements.

The Fe $2p_{3/2}$ peak of the *in situ* film is characterized by a line shape that resembles more that of FePc *ex situ* films. It seems to suggest that the oxidation state of the iron has been altered, Could then the chlorine atom on the central Fe atom in FePcCl be lost and hence the Fe ion passed from Fe(III) to Fe(II)?

In case of the Fe2p line profile the spectrum of *ex situ* FePcCl thin film looks very much like the spectrum of the Fe(II) in *ex situ* FePc (see Figure 5-3). This raises the question if iron atoms in thin *ex situ* prepared layers still are Fe(III) or if the interaction with the substrate alters the oxidation state to Fe(II). For this kind of preparation we should also consider the air contamination of the substrate and of the film (prior transfer of the sample into the vacuum chamber) which could play a quite important role in the adsorption and in the molecule-surface interactions for low coverages.

5.4 *Cl 2p spectra*

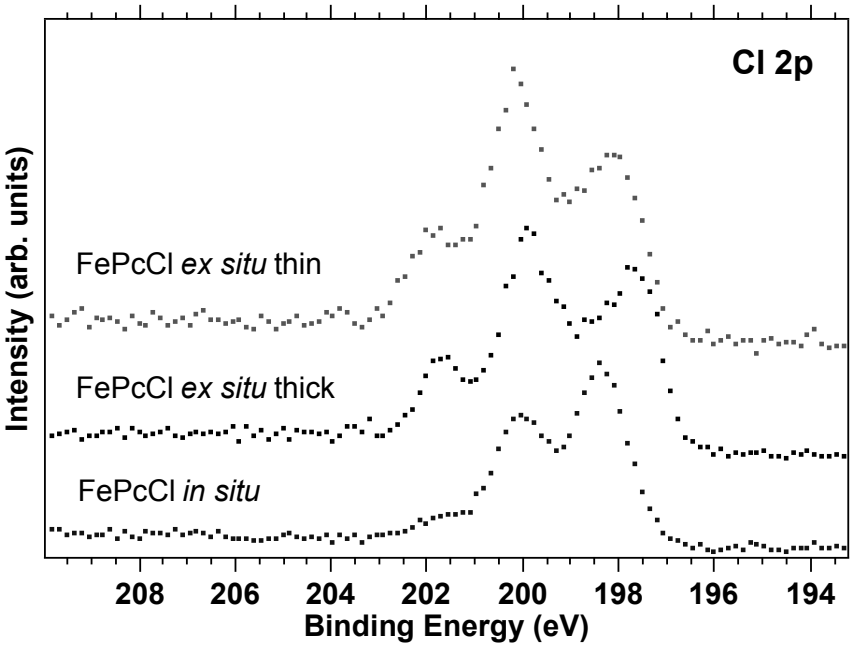

Figure 5-4: Cl 2p XPS spectra

For a chlorine atom the XP spectrum of the Cl 2p level should consist of two components, namely due to the photoemission from the Cl $2p_{1/2}$ and C $l2p_{3/2}$ orbitals[11] and these should be expected for FePcCl, if just one type of Cl atoms would bond to the molecule via the central Fe atom. In Figure 5-4 we observed instead that the Cl 2p spectrum of the *ex situ* samples consists of three features at binding energies around 198.1 eV, 200.2 eV and 201.8 eV. This would indicate the existence of Cl atoms in at least two different chemical environments in

[11] Binding energy for Cl $2p_{1/2}$ = 201 eV and Cl $2p_{3/2}$ = 199 eV according to [22]

the molecular powder. However, the *in situ* sample shows only two spectral components, at 198.4 eV and 200.0 eV binding energies. Obviously, the Cl atoms are not bound to the FePc molecule in the same way after evaporation.

Performing a simple subtraction of the Cl *in situ* double component spectrum (due to the Cl $2p_{1/2}$ and Cl $2p_{3/2}$) from the Cl *ex situ* intensity we can conclude that the three visible peaks are most likely to be four, coming from two similar but chemical shifted chlorine, i.e. characterized by different binding energies (see Figure 5-5). Moreover, the residual intensity after this subtraction (seen in the binding energy region between 197 and 201 eV in Figure 5-5) suggests that we could have still one more double component in between the two used in the fit.

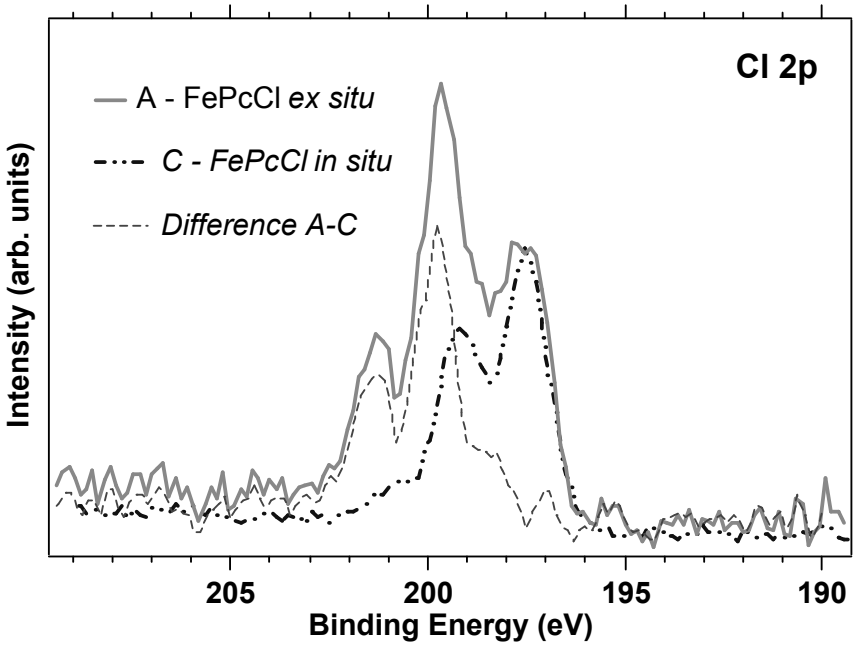

Figure 5-5: A simple subtraction of the Cl *ex situ* and *in situ* components shows that the three peaks for the *ex situ* sample can be decomposed of at least two Cl 2p spectra with an energy shift of 2.2 eV. We also see an extra component with a broad shape and low intensity at the low binding energy side.

The diversity of the spectra for the different preparations evidences that the chlorine is present in different phases/species for *ex situ* and *in situ* depositions. The identification of these different kinds of chlorine is not straightforward. We will discuss this issue in the chapter 7, dedicated to the discussion of the results.

Furthermore, the photoemission results allowed us to estimate the stoichiometry of the molecules deposited on the substrate as powder (*ex situ* samples) and evaporated (*in situ*). For this estimation we considered the relation of the photoemission intensity (area underneath each spectrum) of the Cl 2p, C 1s, Fe 2p lines with respect to the intensity of the N 1s line. Each intensity has been corrected by photoemission cross section of the corresponding line at the photon energy used (1486.7 eV) [23]. Table 5-1 reports the results of this estimation.

x	area	corr. Area	significance	x/N	expected x/N	x
in situ						**in situ**
Cl 2p	25,82	22,65	1,14	0,242	0,125	Cl 2p
C 1s	312,4	312,40	1	3,339	4	C 1s
N 1s	168,4	93,56	1,8	1,000	1	N 1s
Fe 2p3/2	94,04	8,69	10,82	0,093	0,125	Fe 2p
ex situ						**ex situ**
Cl 2p	29,77	26,11	1,14	0,361	0,125	Cl 2p
C 1s	358,1	358,10	1	4,954	4	C 1s
N 1s	130,1	72,28	1,8	1,000	1	N 1s
Fe 2p3/2	81,68	7,55	10,82	0,104	0,125	Fe 2p

Table 5-1: Intensity ratio of the core level lines (C1s, N1s, Fe2p and Cl2p) of FePcCl with respect to the intensity of N1s line for the different kinds of thick molecular films (*in situ* and *ex situ*).

As seen in this table we obtain a significant excess of Cl with respect to N for the *ex situ* prepared film. This indicates that we probably have much more Cl in the powder than expected.

Summarizing, the different results for *ex situ* and *in situ* samples indicate that something happens during the deposition of the *in situ* films. In order to further understand the results a mass-spectrometer was attached to the chamber for monitoring the evaporations. (Read more in chapter 6.)

6 Results and Discussion of Mass Spectrometer Data

The investigation started with a new pocket filled with FePcCl inserted in the evaporator. When UHV was reached the degassing of the pocket by temperature flashing began.

For T flashed up to 120°C, the pressure in the evaporator chamber reached about $1.0*10^{-5}$ mbar.

After the time demanding preliminary degassing procedure, the mass-spectrometer investigation was started. Under slow heating to 100°C significant peaks showed up over the background signal at 2, 17, 18, 28 and 36 relative atomic mass units (amu), identified as reported in Table 6-1.

Amu	composition
2	H_2
17	H_2O
18	H_2O
28	N_2
36	HCl

Table 6-1: The first significant peaks showing up in the mass-spectrometer

Degassing of the pocket continued, reaching temperatures over 340°C five times and a maximum of 355°C once.

After this procedure the pressure in the chamber stayed in the $1*10^{-6}$ mbar region at temperatures around 350°C. Now it was possible to check how pressure would evolve under slower warming, meaning rising from room temperature to 306°C in about 20 min. This process was thoroughly documented with the mass-spectrometer as you can see in Figure 6-1 to Figure 6-5.

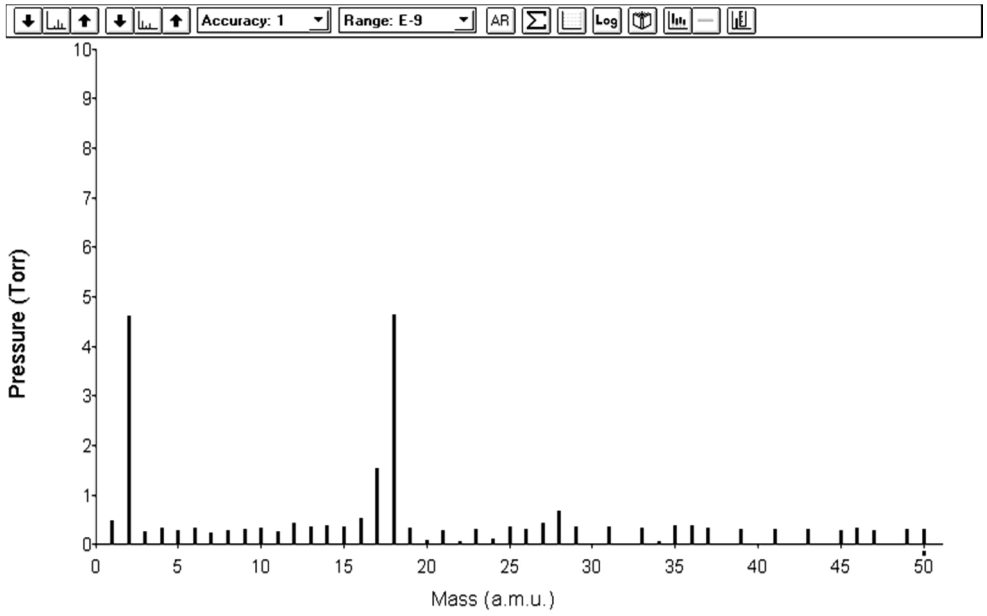

Figure 6-1: A normal background spectra at 23°C. The filament in the mass-spectrometer is warm and not degassing any longer.

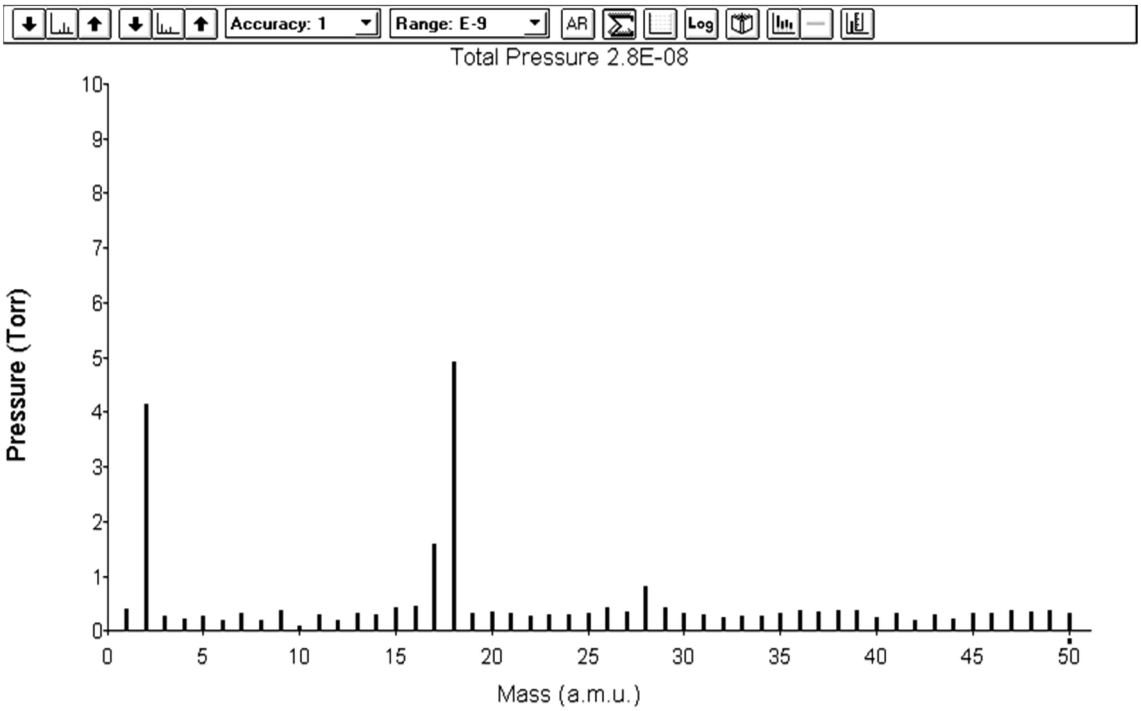

Figure 6-2: Three minutes later. No change in the spectrum at 100 °C compared to room temperature

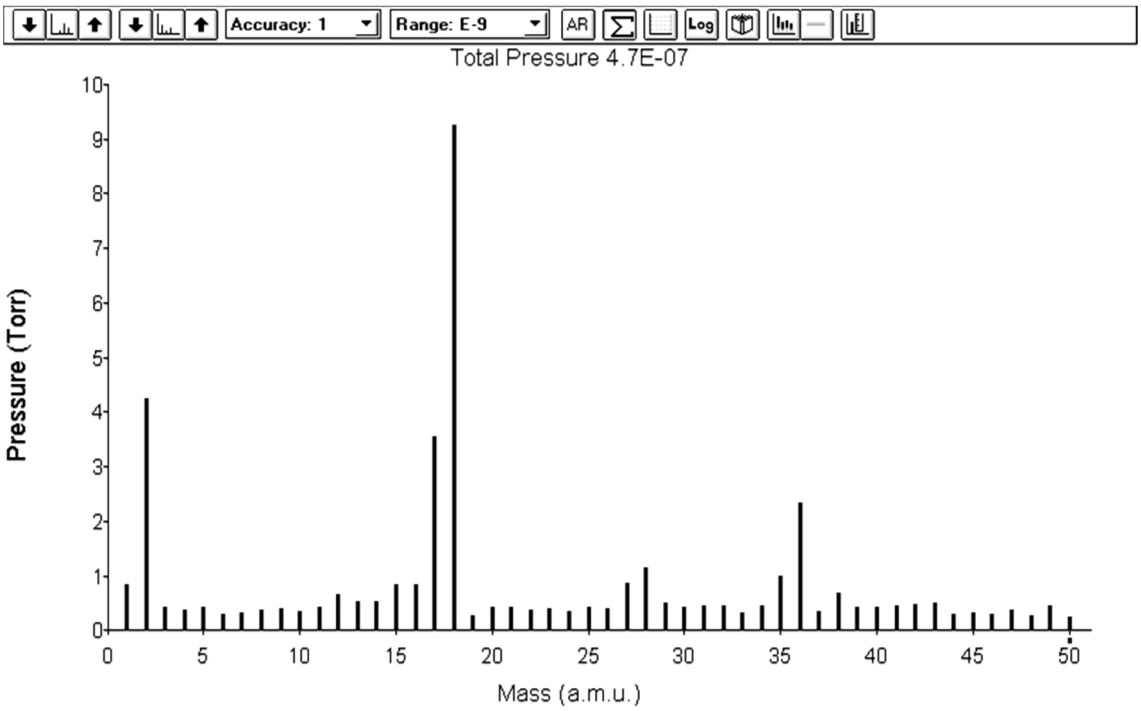

Figure 6-3: Eleven more minutes later at 250°C. No change for H and N, more water. The lines for Cl (at 35 amu) and HCl (36 and 38 amu) start to show up.

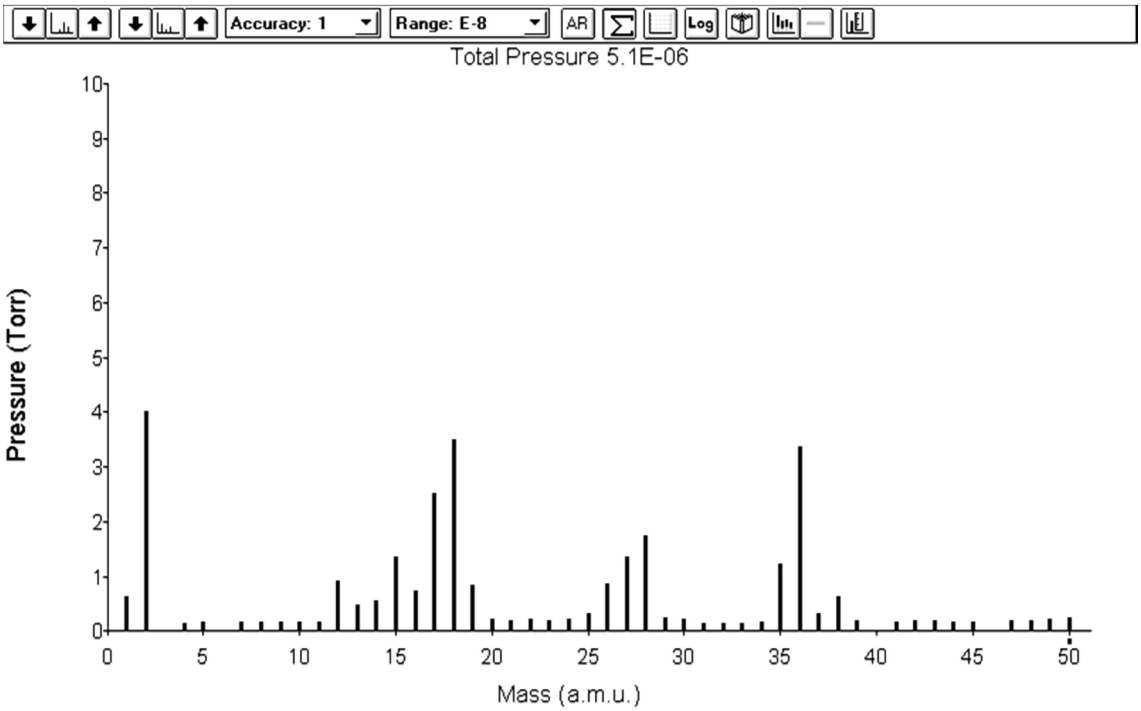

Figure 6-4: After five more minutes at 300°C. A common rise for all lines is observed with increasing HCl and Cl signal.

Amu	Composition
1	H^-
2	H_2
12	C
16	O
17	OH^- (NH_3?)
18	H_2O
28	N_2
28	CO
35	Cl^-
36	HCl
37	Cl^-
38	HCl

Table 6-2: Identification of the lines in Figure 6-4

We can be sure of that the lines at 35 and 37 amu correspond to Cl^- as their size ratio follows the probability ratio for the two stable chlorine ions (see Table 6-3). The same is the case for the lines at 36 and 38 corresponding to HCl.

Cl^{14}	Isotope	Isotopic composition	Relative atomic mass (amu)
	Cl_{35}	75,78%	34,97
	Cl_{37}	24,22%	36,97

Table 6-3: The natural isotopes of chlorine, [24]

H^1	Isotope	Isotopic composition	Relative atomic mass (amu)
	H_1	99,99%	1,01
	H_2 (=D)	0,01%	2,01

Table 6-4: The natural isotopes of hydrogen, [24]

After further degassing the pocket was raised from the evaporation chamber into the bellow and the valve was shut. The evaporation chamber was flooded with nitrogen gas and opened for insertion of the substrates. Under constant flooding the FTO plates were put on a metal grid inside the vacuum chamber. When the evaporation chamber reached UHV again the valve was opened and the pocket lowered to approximately one cm over the substrates. Now the deposition of FePcCl onto the FTO glass plates started.

In Figure 6-5 the evaporation temperature of 350°C is reached and the pressure in the chamber becomes $>2.0*10^{-6}$ mbar.

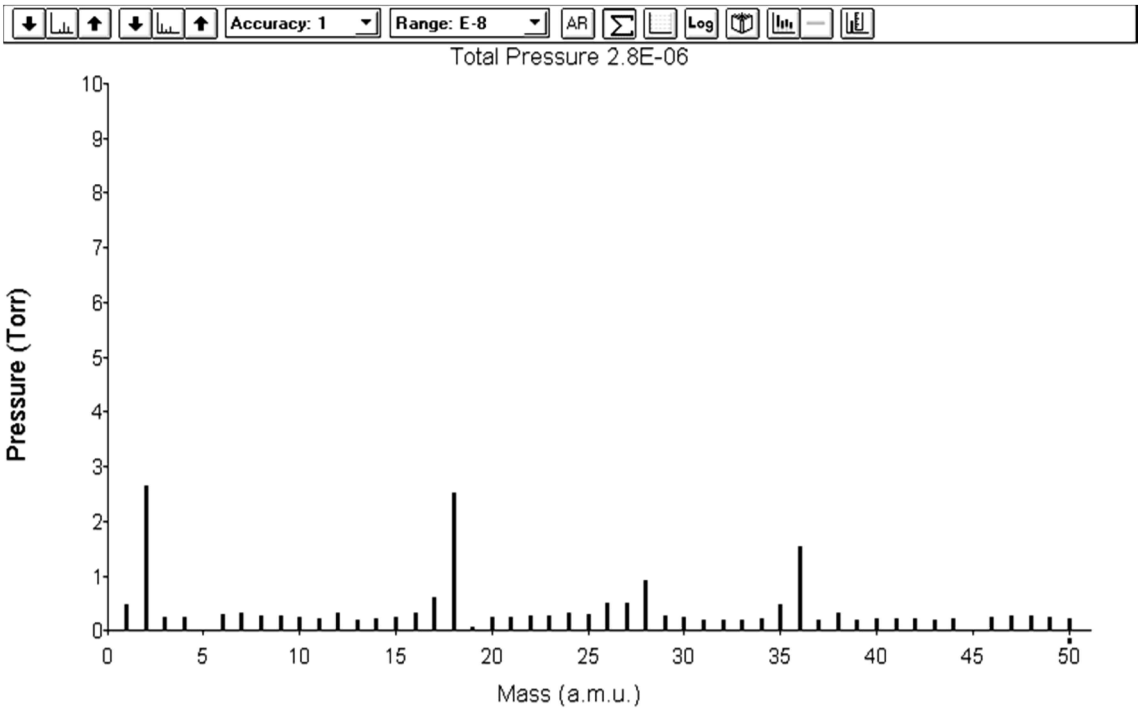

Figure 6-5: The evaporation temperature of 350°C is reached and stable. The deposition of the molecules on the glass substrate will be investigated later by XPS.

Figure 6-6 shows a mass-spectrometer measurement after an evaporation of 16 hours, shortly before the heating was turned off at a pressure of about $5*10^{-7}$ mbar. We noted that the ration between H_20 and HCl/ Cl^- increased. Both peaks are still significantly over the background signal indicating a continuing loss of chloride from the FePcCl-molecules or other residual Cl-complexes present in the molecular powder.

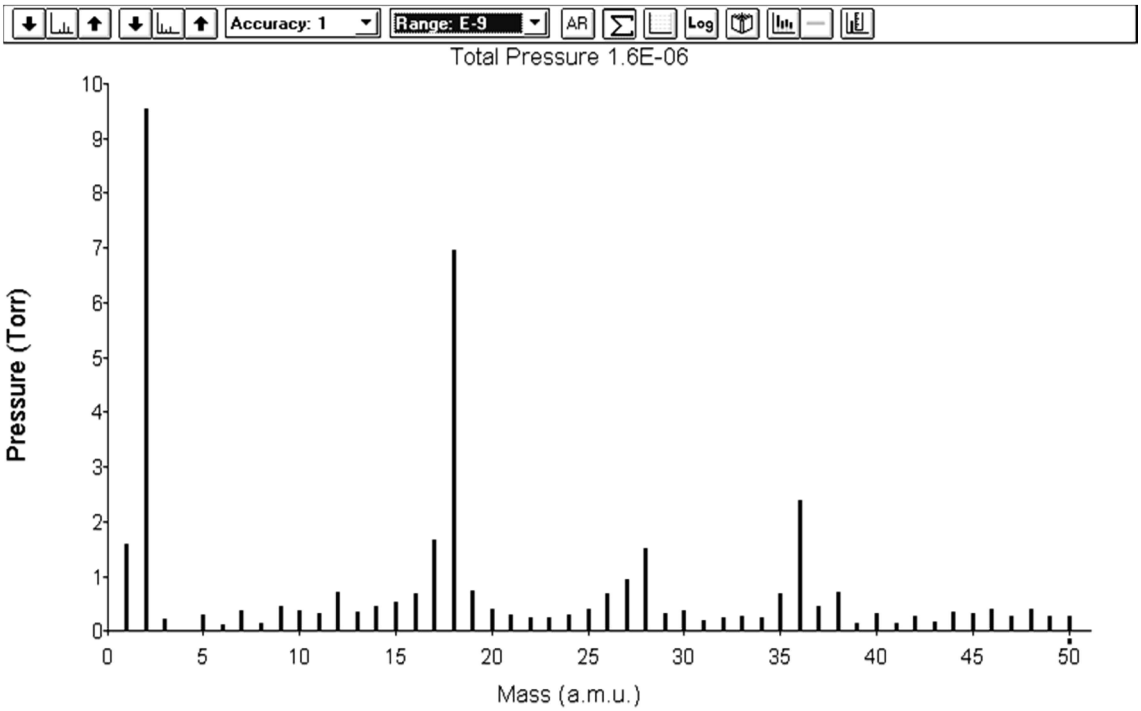

Figure 6-6: After evaporation for 16 hours there is still chlorine left in the vapours.

7 Discussion

The change in line profile of Cl 2p as well as of Fe 2p for in situ and ex situ molecular films of FePcCl, suggests that something happens to the Cl atom ligated to the molecule during evaporation.

The mass spectrometer results clearly indicate that some chlorine leaks out from the powder filled pockets already at very low temperature. The first time Cl was recorded by the mass-spectrometer was at around 80°C when flashing off impurities in the powder. The chlorine observed in the mass spectrometry measurements during our temperature dependent study, could origin from contaminations in the powder, but might also come from the molecules. It is difficult to understand if the chlorine seen in our mass spectroscopy measurements is due (partly or completely) from dissociation of the Cl atom from the Fe atom in the centre of the molecules.

We should consider that the stoichiometric estimations from the XP spectra indicate (both for ex situ and in situ samples) an excess of chlorine with respect to the N atoms of the molecules. This indicates that there is additional Cl or probably Cl-complexes in the powder, releasing Cl when heated. However we cannot exclude that part of the Cl also dissociates from the molecules. This would be supported by the similar Fe 2p spectra of in situ FePcCl and ex situ FePc and by the different Fe 2p spectra for ex situ and in situ FePcCl. We can probably just conclude that what we see is a combination of both cases.

The mass spectroscopic measurements during heating, point at a dissociation temperature for Cl below 250°C. So what happens to the chlorine when FePcCl is evaporated?

Why does the Fe-Cl binding not survive evaporation temperature whilst FePc is a much stable compound at even higher temperatures? As the chlorine is not confined in the molecular structure of the Pc its only neighbour to convey vibrational movements[12] to is the Fe atom. Theoretical calculations show us that the dissociation energy[13] for chlorine-iron porphyrin bond lays around 580K, that is ~ 307°C [25]. This fits well with our observations of chlorine at around 250°C upwards after flashing off impurities.

When the ionised Cl atom (chloride) dissociates from the molecule it is a very aggressive reactant again as all halogens are. It could form Cl_2 gas[14] with other free Cl^- atoms or even detach chloride from another FePcCl molecule. It might attract an H atom and form hydrogen chloride gas[15], HCl which we also saw in the mass spectra.

Another reaction for the Cl^- atoms seemed possible: formation of chlorobenzene. This is a common reaction used for production of colour pigments.

The blue colour pigment phthalocyanine blue BN (see Figure 7-1) looks just like FePc with Cu as central atom instead of Fe.

[12] Due to absorption of heat

[13] Dissociation energy of Cl-ligated Fe porphyrin: E_D ~ 50 meV [25]

[14] Dissociation energy for Cl_2: E_D=2.479 eV [26]

[15] Dissociation energy for HCl: E_D=4.433 eV [26]

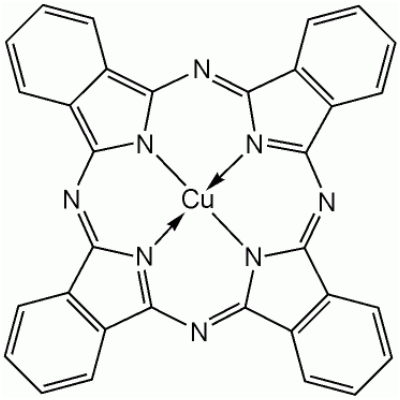

Figure 7-1: Phthalocyanine blue BN [27]

To get different shades of blue and green, chlorine atoms are added to the benzene rings (e.g. Figure 7-2) according to the chemical formula:

$C_{32}\ H_{(x)}\ N_8\ Cl_{(y)}\ Cu$, $(x+y=16)$

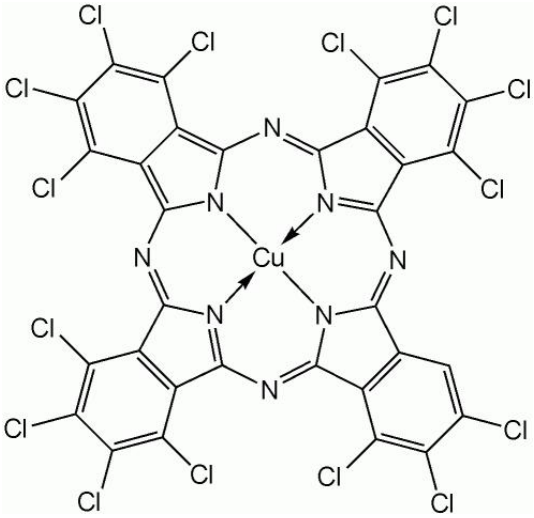

Figure 7-2: Phthalocyanine Green G [28] [16]

A benzene ring has six delocalized π-electrons that attract electron-deficient atoms/ions to the ring but the usual reaction sequence leads to substitution of a hydrogen on the ring by another atom (or group of atoms), as in the synthesis of chlorobenzene. [29] (See Figure 7-3)

[16] Phthalocyanine Green G, also called phthalo green, Pigment Green 7, Copper Phthalocyanine Green, C.I. Pigment Green 42, Non-flocculating Green G, Polychloro copper phthalocyanine, or C.I. 74260, is a synthetic green pigment from the group of phthalocyanine dyes, a complex of copper(II) with chlorinated phthalocyanine. It is a very soft green powder insoluble in water. (...) Its chemical formula ranges from $C_{32}H_3Cl_{13}CuN_8$ to $C_{32}HCl_{15}CuN_8$. (...). The strongly electronegative chlorine atoms influence the distribution of the electrons in the phthalocyanine structure, shifting its absorption spectrum. It is made by chlorination of the phthalocyanine blue as a melt of sodium chloride and aluminium chloride, to which chlorine is introduced at elevated temperature. [19]

$$H_6C_6 + Cl_2 \xrightarrow{catalyst} H_5C_6Cl + HCl$$

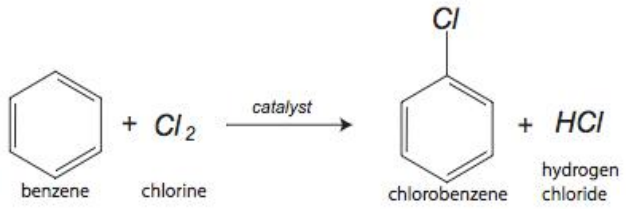

Figure 7-3: The synthesis of chlorobenzene, halogenation of benzene

Here a catalyst is needed to dissociate the diatomic chlorine molecule. However, in our case we do already have free chlorides. Therefore, other possible reactions for the Cl dissociating from the FePcCl molecules could be:

$$H_6C_6 + Cl^- \rightarrow H_5C_6Cl + H^+$$

$$H^+ + Cl^- \rightarrow HCl$$

Even this reaction would result in hydrogen chloride gas, detected by the mass-spectrometer.

To prove the assumption of halogenation of benzene we investigated an *ex situ* sample of iron(II) hexadecachloro phthalocyanine[17], $FePc(Cl)_{16}$ (Figure 7-4). Even that was bought from Sigma-Aldrich who stated a dye content of 80%[18]. Unfortunately the assumption proved to be wrong as the XP spectra of $FePc(Cl)_{16}$ showed a significantly different C1s spectrum (Figure 7-5) even though the Cl 2p spectrum would describe the additional set of Cl 2p peaks in the FePcCl *ex situ* spectra in Figure 5-5 giving rise to the three peak spectrum observed.

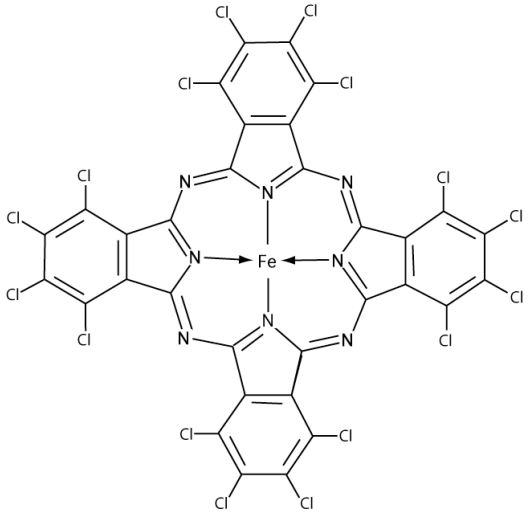

Figure 7-4: Iron(II) hexadecachloro phthalocyanine, $FePc(Cl)_{16}$

[17] chemical formula: C_{32} Cl_{16} Fe N_8
[18] www.sigmaaldrich.com

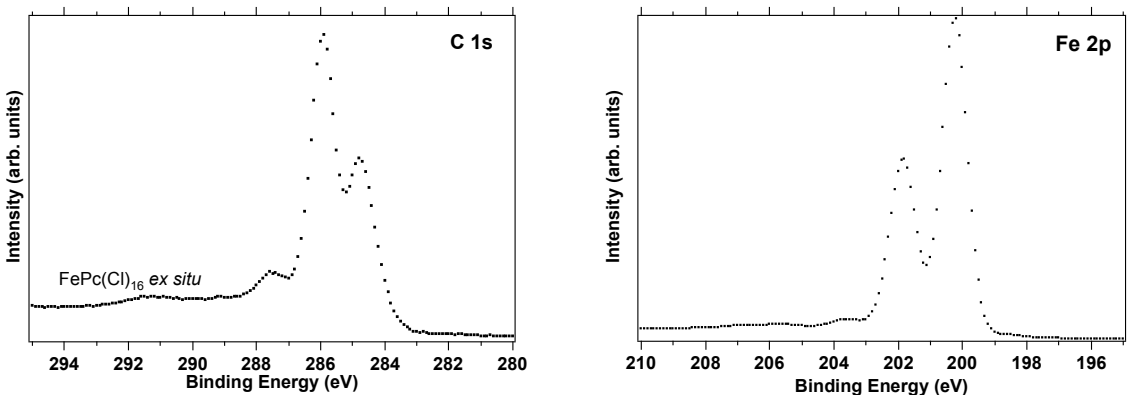

Figure 7-5: C 1s spectrum (left) and Cl 2p spectrum (right) of $FePc(Cl)_{16}$

Probably the most correct interpretation of our results would be to consider the combination of different effects: dissociation but also different molecule-molecule interactions in the film that could give rise to chemical different Cl atoms.

Considering some published works, the reported XP spectrum of Cl 2p for the adsorption of CCl_4 on a single crystal of Fe oxide (namely Fe_3O_4(111)-(2x2) shows a variety of peaks which have been attributed to different molecular species upon adsorption at different surface temperatures.[30][31] Among the different species the $FeCl_2$ would correspond to a Cl 2p two-peak XP spectrum. It is also important to mention that a study on the *in situ* deposition of Boron(III) Sub-phthalocyanine on Ag(111) reported also a two-component Cl 2p XP spectrum to a deposited molecule with still the Cl atom in the molecular centre.[32]

In conclusion we can say that more experiments need to be done to get a deeper understanding on the chemical state of the chlorine observed in the PE spectra of *in situ* FePcCl films.

8 Summary and Conclusions

The aim of this project was to immobilize iron phthalocyanines (FePc and FePcCl) on surfaces and study the electronic structure of the obtained films in relation to the ionic state of the central metal (Fe).

Two different deposition methods have been used and compared, smearing under atmospheric conditions and evaporation in ultra-high vacuum.

We found that Fe(III)PcCl does not seem to be stable enough for evaporation. Our results show that evaporation of FePcCl leads to a clear chlorine signal in the mass spectrum monitoring the deposition. This could be attributed to dissociation of the molecule and/or desorption of Cl in excess (in form of different complexes) present in the molecular powder.

Still there is a chlorine signal in the PE spectra of the molecular films prepared by evaporation. To get knowledge about the chemical state of this chlorine, more experiments need to be done. If the problem of surface charging of the sample during PE investigation can be overcome, the comparison of binding energies at different regions will be able to give valuable information on the chemical states of chlorine and iron in the evaporated samples. A thorough discussion with chemists might also shade more light on the possible chlorine species in the FePcCl powder.

9 Bibliography

[1] S. Berner, S. Biela, G. Ledung et al., vol. 244, no. 1, pp. 86–91, 2006.

[2] A. Braun and J. Tcherniac, *Berichte Dtsch. Chem. Ges.*, vol. 40, pp. 2709, 1907.

[3] H. de Diesbach and E. von der Weid, *Helv. Chim. Acta*, no. 10, pp. 886, 1927.

[4] P. M. Borsenberger and D. S. Weiss, *Organic Photoreceptors for Imaging Systems*. New York: Marcel Dekker, 1993.

[5] J. W. Jinfu Ma, *J. Power Sources*, vol. 172, no. 1, pp. 220–224, 2007.

[6] M. G. Walter, A. B. Rudine, and C. C. Wamser, *J. Porphyr. Phthalocyanines*, vol. 14, no. 09, pp. 759–792, 2010.

[7] M. K. M. S. Roy, *Radiat. Meas.*, vol. 38, no. 2, pp. 205–209, 2004.

[8] H. Kolarova, K. Tomankova, R. Bajgar et.al., *Ultrasound Med. Biol.*, vol. 35, no. 8, pp. 1397–1404, 2009.

[9] M. Yoshida, K. Suemori, S. Uemura et.al., *Mol. Cryst. Liq. Cryst.*, vol. 471, no. 1, pp. 21–27, 2007.

[10] C. E. Dent, R. P. Linstead, and A. R. Lowe, *J. Chem. Soc. Resumed*, pp. 1033–1039, 1934.

[11] M. K. Engel, *Kawamura Rikagaku Kenkyusho Hokoku*, no. 8, pp. 11–54, 1997.

[12] F. Iwatsu, *J. Phys. Chem.*, vol. 92, no. 6, pp. 1678–1681, 1988.

[13] E. Sokolowski, C. Nordling, and K. Siegbahn, "Magnetic analysis of x-ray produced photo and auger electrons," *Ark. Fys.*, vol. 12, pp. 301–318, 1957.

[14] C. Nordling, E. Sokolowski, and K. Siegbahn, *Phys. Rev.*, vol. 105, no. 5, pp. 1676–1677, 1957.

[15] J. Schweppe, R. Deslattes, T. Mooney, and C. Powell, *J. Electron Spectrosc. Relat. Phenom.*, vol. 67, no. 3, pp. 463–478, 1994.

[16] Y. Alfredsson, J. Ahlund, K. Nilson et.al., *Thin Solid Films*, vol. 493, no. 1–2, pp. 13–19, 2005.

[17] M. S. Liao and S. Scheiner, *J. Chem. Phys.*, vol. 114, no. 22, pp. 9780–9791, 2001.

[18] J. Ahlund, K. Nilson, J. Schiessling et.al., *J. Chem. Phys.*, vol. 125, no. 3, p. 034709, 2006.

[19] Y. Alfredsson, B. Brena, K. Nilson et.al., *J. Chem. Phys.*, vol. 122, no. 21, p. 214723, 2005.

[20] B. Brena, C. Puglia, M. de Simone et.al., *J. Chem. Phys.*, vol. 134, no. 7, p. 074312, 2011.

[21] "XPS Interpretation of Iron." [Online]. Available: http://xpssimplified.com/elements/iron.php. [Accessed: 26-Jun-2015].

[22] J. F. Moulder, W. F. Stickle, and P. E. Sobol, *Handbook of X-ray photoelectron spectroscopy*. Perkin-Elmer Corporation, 1992.

[23] J. H. Scofield, *J. Electron Spectrosc. Relat. Phenom.*, vol. 8, no. 2, pp. 129–137, 1976.

[24] N. US Department of Commerce, "NIST: Atomic Weights and Isotopic Compositions of the Elements." [Online]. Available: http://www.nist.gov/pml/data/comp.cfm. [Accessed: 09-Jun-2015].

[25] "Private communication with Poogia Panchmatia and Peter Oppeneer, Dept. of Physics, Theoretical Magnetism group, Uppsala universitet."

[26] G. Herzberg, *Molecular spectra and molecular structure*. New York: Van Nostrand, 1950.

[27] "Phthalocyanine," *Wikipedia, the free encyclopedia*. 26-May-2015.

[28] "Phthalocyanine Green G," *Wikipedia, the free encyclopedia*. 03-Jun-2014.

[29] "organohalogen compound :: Preparation -- Britannica Online Encyclopedia." [Online]. Available: http://academic.eb.com.ezproxy.its.uu.se/EBchecked/topic/431995/organohalogen-compound/277960/Preparation?anchor=ref1000173. [Accessed: 09-Jun-2015].

[30] K. Adib, N. Camillone III, J. P. Fitts, K. T. Rim, G. W. Flynn, S. A. Joyce, and R. M. Osgood Jr, *Surf. Sci.*, vol. 497, no. 1–3, pp. 127–138, 2002.

[31] K. Adib, D. R. Mullins, G. Totir, N. Camillone III, J. P. Fitts, K. T. Rim, G. W. Flynn, and R. M. Osgood Jr., *Surf. Sci.*, vol. 524, no. 1–3, pp. 113–128, 2003.

[32] S. Berner, M. de Wild, L. Ramoino, S. Ivan, A. Baratoff, H.-J. Güntherodt, H. Suzuki, D. Schlettwein, and T. A. Jung, *Phys. Rev. B*, vol. 68, no. 11, p. 115410, 2003.